The 8th European Congress on Computational Methods in Applied Sciences and Engineering
ECCOMAS Congress 2022
5-–9 June 2022, Oslo, Norway

A SIMPLE DIFFUSE INTERFACE STRATEGY FOR MULTIMATERIAL DIFFUSION EQUATION.

B. Manach-Pérennou[1], R. Chauvin[1], S. Guisset[1], J.P. Perlat[1]

[1] CEA, DAM, DIF, F-91297 Arpajon, France.
e-mail: bastien.manach-perennou@cea.fr

Key words: Multimaterial flows, diffuse interface, diffusion equation.

Abstract. The present document is motivated by the development and the study of diffuse interface strategies which does not require the use of geometric interface reconstructions. A simple diffuse interface strategy is proposed for the multimaterial diffusion equation. While it is possible to consider only one average temperature per mixed cell, it is known [7] that standard harmonic or arithmetic homogeneous methods are not accurate on the simple "sandwich" problem when working with coarse meshes. This has direct consequences for radiation-hydrodynamics applications. The numerical strategy presented here may be seen as a natural extension of standard homogeneous model and understood as if the diffusion operator is integrated on the global cell (not the materials) taking into account several temperature (one per material). Obviously, the accuracy of the presented method, compared to exact geometric reconstruction based ones, is expected to be lower in the general case. However, we believe that the simplicity of the methodology introduced in the present document, its robustness and practicality for real physical applications makes it interesting for a large audience.

1 INTRODUCTION

Multiphase flows arise in various engineer applications. However, the numerical treatment of discontinuities between separated phases, while avoiding spurious oscillations and enforcing thermodynamics consistency is a challenging issue. Over the years, two main categories of method have emerged in order to handle multiphases interface. The first one which does not allow any phase mixing is often referred as sharp interface methods [9, 5] while the second one deals with interface as a diffused area in which the interface is not clearly defined. These methods are often referred to as diffused interface methods. In the first category falls standard front tracking methods [5, 11] and Lagrangian methods [2] for which the mesh is adapted (or naturally adapts) to follow the material interface. In this group, one may also find several methods based on reconstruction techniques, such as the one proposed in [10]. On the other hand, diffuse interface methods have been largely explored over recent years. These methods allow a diffuse mixing region of fluids. Early ideas were introduced in [3]. Then another class of diffuse interface methods have emerged, starting with the works performed in [6]. More recently, based on these ideas, Baer-Nunziato type models [1] are considered for various applications. A known drawback of the diffuse interface methods comes from the smearing of the interface. However, this point may be mitigated with standard anti-diffusive (diffusion-sharpening) strategies. Comparing this drawback which its great advantages: a single system applied on the whole domain excluding

geometric reconstruction or interface tracking and a large flexibility for multi-physics coupling extensions, it makes the approach particularly attractive. Here, we refer to [8], for a clear review of the numerical methods used in this context. In Figure 1 is displayed the different strategies encountered in literature for the treatment of discontinuities between separated phases. In the

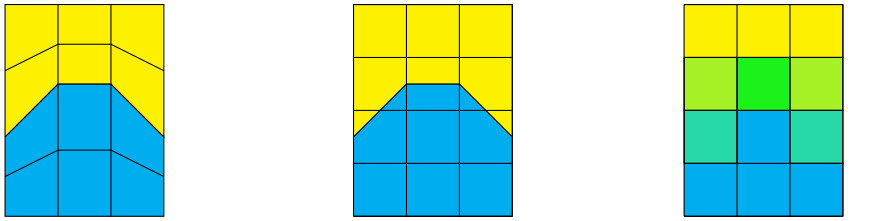

Figure 1: Illustration of different strategies for the treatment of discontinuities between separated phases.

present study, we will focus on the numerical resolution of the multimaterial heat equation. Multiple non-miscible materials i are considered, each of them being described locally by the heat equation

$$c_v^i \rho^i \partial_t T^i + \nabla \left(\kappa^i \nabla T^i \right) = 0.$$

The numerical treatment of multimaterial diffusion problems is challenging because of the spatial discretization of the diffusion operator in mixed cells (i.e. cells in which multiple material cohabit). As a matter of fact, the spatial integration of this operator naturally leads, using the Stokes' formula, to evaluate fluxes interfaces. However, this supposes the knowledge of the position of all the materials in the mixed cells. This information is, in general, not directly available and may require exact or approximate interface reconstructions between materials inside a mixed cell. Despite the large literature on the subject, efficient numerical geometric surface reconstruction is still hard to achieve in practice. Indeed, the algorithm required is relatively "fastidious" especially in the presence of several materials in a 2D or 3D context. In addition, the reconstruction procedures are sometimes very costly from a numerical point of view since the method may not be naturally suitable for large parallel computing. Even worse, geometric reconstructions may also strongly impact the numerical convergence of the iterative method used (in general a standard conjugate gradient method is used for diffusion problems). The robustness of the overall method may also be affected (especially in the presence of small volume fraction). These remarks motivate the development and the study of diffuse interface strategies which do not require the use of geometric interface reconstructions. This constitutes the purpose of the present document, in which a simple diffuse interface strategy is proposed for the multimaterial diffusion equation. Obviously, the accuracy of the presented method, compared to exact geometric reconstruction based ones, is expected to be lower in the general case. However, we believe the simplicity of the methodology introduced in the present document, its robustness and practicality for real physical applications makes it interesting for a large audience.

While it is possible to consider only one average temperature per mixed cells, it is known [7] that standard harmonic or arithmetic homogeneous methods are not accurate on the simple "sandwich" problem when working with coarse meshes. This has direct consequences for

radiation-hydrodynamics applications. Indeed, in strongly coupled regimes, a radiative temperature in each material inside a mixed cell is then mandatory to avoid an artificial heating (or cooling) of a material with respect to the other. As it will be explained in details, the numerical strategy presented here may be seen as a natural extension of standard homogeneous model and understood as if the diffusion operator is integrated on the global cell (not the materials) taking into account several temperature (one for each material).

The document is organized as follows. Standard homogeneous methods are first recalled and the principle of the diffuse interface strategy is detailed. The computation of the surface proportions is then detailed followed by the practical computation of the fluxes. Finally, the diffuse interface strategy is confronted to homogeneous ones with two test cases.

2 Presentation of the methods

Throughout this section, we will consider the so-called sandwich problem [7] as a way to illustrate each method and compare them to one another. Its layout is as follows: a first material α encircles a second material β as described in Figure 2. Thermal conductivities are assumed to be a constant scalar for each material ($\kappa^\alpha = 0$ and $\kappa^\beta = 1$). The bottom and top bounds of the domain are thermostats at respective temperatures T_1 and T_2. The heat flux is assumed to be zero at the left and right borders. In particular, we look at a square mixed cell of length h divided vertically in two by the interface between materials α and β. The interface is assumed to lie in the middle of the cell so that the volume fractions of the materials are both equal to $\frac{1}{2}$. The geometry of the system is summarized on Figure 2. The surfaces temperatures and directional fluxes ω are identified with the subscripts l (left), r (right), b (bottom) and t (top). The approximated incoming fluxes are

$$\omega_l^\alpha = 0, \qquad \omega_b^\alpha = 0, \qquad \omega_l^\beta = 0, \qquad \omega_b^\beta = \frac{1}{2}\frac{T_b^\beta - T^\beta}{h/2},$$

$$\omega_r^\alpha = 0, \qquad \omega_t^\alpha = 0, \qquad \omega_r^\beta = \frac{T_r^\beta - T^\beta}{h/4}, \qquad \omega_t^\beta = \frac{1}{2}\frac{T_t^\beta - T^\beta}{h/2}.$$

These fluxes will be compared with the fluxes derived from the methods presented henceforth.

2.1 Homogeneous methods

Homogeneous methods are one of the simplest methods one may think of. Mixed cells are assumed to contain a fictive single material whose thermal conductivity is an average of the thermal conductivities of the real materials. Here, we consider the homogenized material is described by a single scalar: the equivalent conductivity. Several choices are possible in order to compute this conductivity: here, harmonic and arithmetic means are considered, both weighted by the volume fraction of the materials. Coming back to the sandwich problem and the previously described mixed cell, volume fractions are equal and we define two thermal conductivities for the mixture

$$\kappa_A = \frac{1}{2}\left(\kappa^\alpha + \kappa^\beta\right) = \frac{1}{2}, \qquad \kappa_H = \frac{2}{1/\kappa^\alpha + 1/\kappa^\beta} = 0.$$

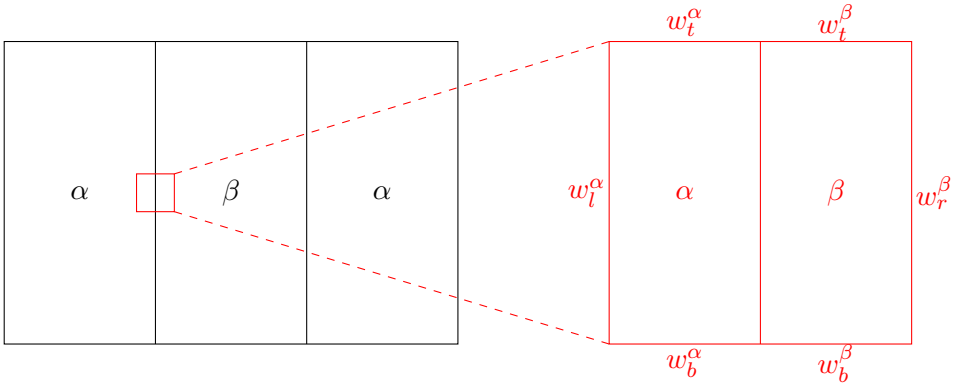

Figure 2: sandwich problem layout (black) and mixed cell of interest (red).

We now write the fluxes at each face of the cell. Because only the mixture material is considered, there is only one common flux at each face for both materials. For the arithmetic mean one founds

$$w_l = \frac{1}{2}\frac{T_l - T}{h/2}, \qquad w_b = \frac{1}{2}\frac{T_b - T}{h/2}, \qquad w_r = \frac{1}{2}\frac{T_r - T}{h/2}, \qquad w_t = \frac{1}{2}\frac{T_t - T}{h/2}.$$

All fluxes are non-zero which is not physically correct when material α is involved. As for material β, the vertical fluxes are correct but the right one is weaker than it should be. For the harmonic mean we have

$$w_l = 0, \qquad w_b = 0, \qquad w_r = 0, \qquad w_t = 0.$$

All fluxes are null, which makes sense for material α but not for material β. Both examples hence show that the isotropic mixture material hypothesis cannot allow coherent fluxes for both materials: fluxes are either overvalued or undervalued.

2.2 Diffuse interface strategies

On the aforementioned example, homogeneous methods do not seem to be able to capture accurately all fluxes at once. Hence, we now assume that each material has its own temperature inside the cell. Fluxes are then computed between pairs of materials. The number of temperatures and fluxes is significantly larger than in the homogeneous case. The addition of these new degrees of freedom is expected to allow a more accurate computation of fluxes. The methodology presented here extends the work presented in [4].

2.2.1 Principle

Considering a mixed cell c and assuming that the position of each material is known (with an interface reconstruction technique for example), we may integrate the heat equation on each material sub-volume leading to

$$\int_{V^{\alpha_c}} \partial_t T dv = \int_{\partial V^{\alpha_c}} (D\nabla T) \cdot \vec{n} ds.$$

Then dividing the surface ∂V^{α_c} into sub-surfaces $(\partial V^{\alpha_c})^{\beta_d}$ where the material α of cell c is in contact with the material β of cell d (it is not excluded that $c = d$), we may write

$$\int_{V_c^\alpha} \partial_t T dv = \sum_{\beta_d} \int_{(\partial V^{\alpha_c})^{\beta_d}} (D\nabla T) \cdot \vec{n} ds = \sum_{\beta_d} w^{\alpha_c \beta_d}. \tag{1}$$

Notice that the sum may be taken over all materials of all cells by defining arbitrarily $w^{\alpha_c \beta_d} = 0$ when both materials are not in contact. In our case, no information concerning the geometry of the mixed cell is known. In particular, the position of each material inside the cell and their surface of contact at each interfaces with neighbor cells is not known. Nevertheless, we may still want to mimic the interface reconstruction formulation, write equation (1) and come up with an expression of the fluxes $w^{\alpha_c \beta_d}$. In this diffuse interface framework, the only non-zero fluxes are assumed to be between materials belonging to neighbor cells (i.e. cells c and d sharing a common face). Then, for the time being, fluxes between same-cell materials are set to zero. As for the non-zero fluxes, they are expressed as follows

$$w^{\alpha_c \beta_d} = k^{\alpha_c} \frac{T^{\alpha_c \beta_d} - T^{\alpha_c}}{h/2} f^{\alpha_c} f^{\beta_d}, \tag{2}$$

where $T^{\alpha_c \beta_d}$ is the temperature at the interface between material α of cell c and material β of cell d. This strategy may be seen as a natural extension of the homogeneous ones since

- it is considered that all materials in a mixed cell "exchange" with all the materials in the neighbor cells.
- the "exchange" surface proportion are shared according to the material in the mixed cell. This choice will be discussed in the next section. The simplest choice consists in considering the volume fraction of each material. This constitutes a simple conservative extension of the standard homogeneous model.
- the diffusion coefficient discretization follows the homogeneous case and is simply an average of each diffusion coefficient of the material in the mixed cell.

Remarks. As for the homogeneous methods, the flux inside the mixed cell is not an unknown of the problem. In addition, it must be pointed out that the materials inside two neighbor cells only see each other by pair while the materials inside a mixed cell does not see each other directly. This point is illustrated in Figure 3 where the dashed lines displayed the fact that materials inside a mixed cell does not see each other directly.

Coming back to the sandwich problem, fluxes through the mixed cells are computed with the relationship $w_d^\alpha = \sum_\beta w^{\alpha_c \beta_d}$ with $d \in \{b, t, l, r\}$ (for readability purposes, we do not differentiate neighbor cells and the faces they share with the central cell) which yields

$$\omega_l^\alpha = 0, \qquad \omega_b^\alpha = 0, \qquad \omega_l^\beta = 0, \qquad \omega_b^\beta = \frac{1}{4} \frac{T_b^\beta - T^\beta}{h/2},$$

$$\omega_r^\alpha = 0, \qquad \omega_t^\alpha = 0, \qquad \omega_r^\beta = \frac{1}{2} \frac{T_r^\beta - T^\beta}{h/2}, \qquad \omega_t^\beta = \frac{1}{4} \frac{T_t^\beta - T^\beta}{h/2}.$$

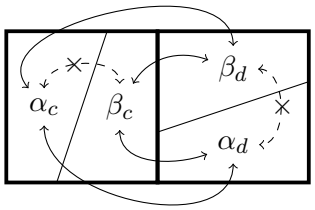

Figure 3: Illustration of the exchange between materials of a cell c (left part) and materials inside a cell d (right part). The dashed lines displayed the fact that materials inside a mixed cells does not see each other directly. The continuous lines show that all materials in a cell exchange with the materials in the neighbor cell.

Because fluxes are separated for each material, this method gives physically more relevant results. Indeed, all fluxes related to material α are null as its thermal conductivity is zero but conduction phenomena involving material β are still captured. However, because of the simplicity of this model, we cannot expect to compute correct fluxes for all possible geometric configurations. In our case, for material β, the left flux is correct, but the others are undervalued. For the top and bottom fluxes, material β is only in contact with itself, but the model considers that half of the surface is shared with material α so that the resulting flux is half of its real value. This consideration still holds for the right flux, which is further weakened by the misplacement of the center of the material volume which does not coincide with the center of the cell, resulting in a flux 4 times smaller than its expected value.

2.2.2 Computation of the surface proportions

When computing the diffusive interface strategy fluxes pairs by pairs, we assume that materials α_1 and β_2 share a contact zone which represents a proportion $p^{\alpha_1\beta_2} = f_1^\alpha f_2^\beta$ of the total face surface. Here, we investigate other ways of defining these proportions. We assume that the total proportions at the interface on each side $f_+^{\alpha_1}$ and $f_-^{\beta_2}$ are known for each material α and β. We want to estimate the proportions $p^{\alpha_1\beta_2}$ with the constraints:

$$\begin{cases} \displaystyle\sum_{\beta_2} p^{\alpha_1\beta_2} = f_-^{\alpha_1} & \forall \alpha_1, \\ \displaystyle\sum_{\alpha_1} p^{\alpha_1\beta_2} = f_+^{\beta_2} & \forall \beta_2. \end{cases}$$

For two materials, it gives us four equations and four indeterminates. The underlying linear application is not bijective, its image only being of dimension 3. Its image (i.e. the set of coefficients $(f_-^\alpha, f_+^\alpha, f_-^\beta, f_+^\beta)$ for which solutions exist) is the hyperplane $f_-^\alpha + f_-^\beta = f_+^\alpha + f_+^\beta$. By construction, our coefficients satisfies this equality so that solutions exists. The set of solutions is an affine space given by a particular solution (e.g. the one given by the diffusive interface strategy) and the kernel (which is the line spanned by $p^{\alpha_1\alpha_2} = 1$, $p^{\alpha_1\beta_2} = -1$, $p^{\beta_1\alpha_2} = -1$ and

$p^{\beta_1\beta_2} = 1$). Finally, solutions are of the form

$$\begin{cases} p^{\alpha_1\alpha_2} = f_+^\alpha f_-^\alpha + \lambda, \\ p^{\alpha_1\beta_2} = f_+^\alpha f_-^\beta - \lambda, \\ p^{\beta_1\alpha_2} = f_+^\beta f_-^\alpha - \lambda, \\ p^{\beta_1\beta_2} = f_+^\beta f_-^\beta + \lambda. \end{cases}$$

In order to ensure that every proportion stays between 0 and 1, the following inequalities must hold

$$-\min(f_+^\alpha f_-^\alpha, f_+^\beta f_-^\beta) \leq \lambda \leq \min(f_+^\alpha f_-^\beta, f_+^\beta f_-^\alpha).$$

In our numerical applications, we will distinguish three extreme cases:

- $\lambda = 0$ which gives back the classical diffusive interface strategy. This choice will be referred to as "neutral".
- $\lambda = -\min(f_+^\alpha f_-^\alpha, f_+^\beta f_-^\beta)$ which maximizes the surface between pairs of different materials (namely (α_1, β_2) and (β_1, α_2)). This choice will be referred to as "min".
- $\lambda = \min(f_+^\alpha f_-^\beta, f_+^\beta f_-^\alpha)$ which minimizes the previously mentioned surfaces (hence maximizing the surfaces between the couples (α_1, α_2) and (β_1, β_2)). This choice will be referred to as "max".

These different adjustments may be visualized on Figure 4.

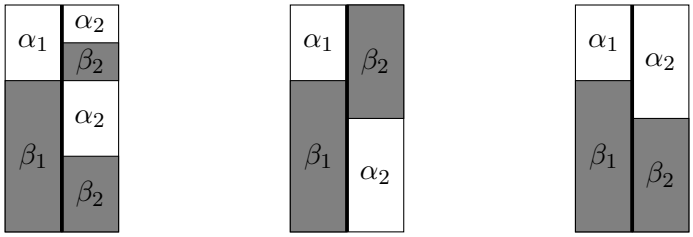

Figure 4: Visualization of the neutral (left), min (center) and max (right) cases for given total proportions. On each scheme, the bold line corresponds to the interface. As an example, the proportion $p^{\alpha_1\beta_2}$ is the ratio of the surface shared by rectangles α_1 and β_2 on the total surface of the interface (i.e. $\frac{1}{6}$ for neutral, $\frac{1}{3}$ for min and 0 for max).

2.2.3 Computation of the surface volume fractions and internal flux

We now discuss the computation of the surface volume fractions $f_+^{\alpha_1}$ et $f_-^{\alpha_2}$. In our numerical applications, two choices will be considered:

- Constant reconstruction: $f_+^{\alpha_1}$ simply takes the cell value f^{α_1}.
- Linear reconstruction: $f_+^{\alpha_1}$ is computed thanks to the cell gradient ∇f^α which depends itself on a limiter.

Figure 5: One mixed cell ($f^\alpha = f^\beta = \frac{1}{2}$) surrounded by two pure cells. Between the left and middle cells, the face volume fractions are: $f^\alpha_+ = \frac{1}{2}$ (constant) and $f^\alpha_+ = \frac{1}{4}$ (linear).

The linear reconstruction of the surface proportions is expected to be closer to the geometry of the problem layout. However, such choice is quite incompatible with the basics of the diffuse interface strategy as shown with the example depicted on Figure 5. Here, linear reconstruction gives lower surface proportions between different materials. The new surface proportions are closer to the real ones, which are null, but because the diffusive interface strategy does not take into account any flux between materials belonging to the same cell, the overall flux through the mixed cell is seriously undervalued. Hence, linear reconstruction calls for an added flux between materials inside the cell: such flux will be referred to as an internal flux. Concerning the computation of the internal flux, the technical details of the internal surface and internal length (distance between the center of gravity of the respective domain) are not given here but can be computed exactly in this 2D context.

2.3 Practical computation of the flux

All of the above-written fluxes are expressed in terms of surface temperatures. Instead of directly approximating these temperatures, we now use equivalent thermal conductivities that enable us to write the fluxes without surface temperatures.

2.3.1 Textbook case: flux through a two layers wall

Let us consider a wall of surface S and made of two layers of same width $h/2$ and respective thermal conductivities κ_1, κ_2. Temperatures T_1 and T_2 are imposed on both sides of the wall and the flux is assumed null at the top and bottom borders of the wall. The problem is one-dimensionnal and T_s is the temperature at the interface. If we assume that the problem is stationary, then the flux $S\omega$ is constant along the width of the wall. The surface flux ω is given by $\omega = \kappa_1 \partial_x T$ inside the first layer and $\omega = \kappa_2 \partial_x T$ inside the second layer. After integration on their respective domain, these equations yield

$$T_s = \frac{\kappa T_1 + \kappa_2 T_2}{\kappa_1 + \kappa_2}, \qquad \omega h = \frac{2\kappa_1 \kappa_2}{\kappa_1 + \kappa_2}(T_2 - T_1).$$

The coefficient $\frac{2\kappa_1\kappa_2}{\kappa_1+\kappa_2}$ acts as an equivalent thermal conductivity which enables us to bypass the use of the surface temperatures. For the homogenization methods, there is only one thermal conductivity per cell so that this methodology may directly be applied. Hence, at each face, the flux is computed thanks to this equivalent thermal conductivity. The new expressions cannot be exact because the problem may not be stationary nor one-dimensionnal; yet, it could still be physically relevant.

2.3.2 4-temperature diffusive interface strategy

As for the diffusive interface strategy, we may try to use the same methodology developed above to write all fluxes without the surface temperatures. We consider two adjacent cells 1 and 2 each containing two materials α and β. All physical quantities are identified with a subscript indicating the cell to which it belongs and a superscript regarding the material it is related to. We may assume that there are 4 different temperatures $T^{\alpha_1\alpha_2}, T^{\alpha_1\beta_2}, T^{\beta_1\alpha_2}$ and $T^{\beta_1\beta_2}$ at the interface: one for each surface of contact between a material of cell 1 and another of cell 2. If we assume that the four fluxes between each couple of materials are independent of one another, we may replicate the computations of section 2.3.1 separately for each flux. Hence, we get the following expressions

$$\omega^{\alpha_1\alpha_2} = \frac{2\kappa_1^\alpha\kappa_2^\alpha}{\kappa_1^\alpha+\kappa_2^\alpha}\frac{T_2^\alpha-T_1^\alpha}{h}f_1^\alpha f_2^\alpha, \qquad \omega^{\alpha_1\beta_2} = \frac{2\kappa_1^\alpha\kappa_2^\beta}{\kappa_1^\alpha+\kappa_2^\beta}\frac{T_2^\beta-T_1^\alpha}{h}f_1^\alpha f_2^\beta,$$

$$\omega^{\beta_1\alpha_2} = \frac{2\kappa_1^\beta\kappa_2^\alpha}{\kappa_1^\beta+\kappa_2^\alpha}\frac{T_2^\alpha-T_1^\beta}{h}f_1^\beta f_2^\alpha, \qquad \omega^{\beta_1\beta_2} = \frac{2\kappa_1^\beta\kappa_2^\beta}{\kappa_1^\beta+\kappa_2^\beta}\frac{T_2^\beta-T_1^\beta}{h}f_1^\beta f_2^\beta.$$

3 Numerical results

3.1 1D problem: multilayered wall

We begin by looking at a simple 1D problem where the flux is orthogonal to the interfaces between materials. We consider the domain $[0,1]\times[0,0.1]$ divided into 8 equal parts along the x-axis. The first material of thermal conductivity 1 occupies the first, third, fifth and seventh parts; the second material of thermal conductivity 0.01 occupies the rest of the domain. Temperature is set to $T_l = 4$ at the left, and $T_r = 0$ at the right. Fluxes are set to zero along the top and bottom borders. In terms of discretization, a $N_x \times 1$ mesh is considered. Results at $t = 1$ of the different mixed cell strategies and different values of N_x are then compared with a reference solution obtained with a 1×8000 mesh which only contains pure cells. For every pair of adjacent cells, at least one of them is a pure cell: no adjustment is possible so that we only consider the neutral case for the 4-temperatures method. On Figure 6, the log-error between the reference and the arithmetic homogeneous mean is plotted for different sizes of mesh. The plot does not consist in a straight line, but rather in a curve on which a pattern is repeated along a straight line. The pattern depends on the geometry of the problem: here, volume fractions inside mixed cells only depend on the value of N_x modulo 8 (in particular, if $N_x \equiv 0[8]$, no mixed cells are present and all methods are equivalent.). As a result, methods may be compared on two different levels. Setting the volume fractions inside mixed cells (by working with a constant N_x modulo 8) one may study the convergence of each method as it is done on Figure 6 with $N_x \equiv 2[8]$. The order of convergence of the different methods seems to be practically the same for fixed values of N_x modulo 8 (this is not surprising, as they are all equivalent for $N_x \equiv 0[8]$). Alternatively, and more interestingly, one may study the patterns themselves in order to compare different methods on a local approach and hence evaluate the effect of mixed cells on the solution (see Figure 7).
Significant differences may be observed when considering the modulated patterns. For low values of N_x, the linear reconstruction method with internal flux is the most accurate one: the

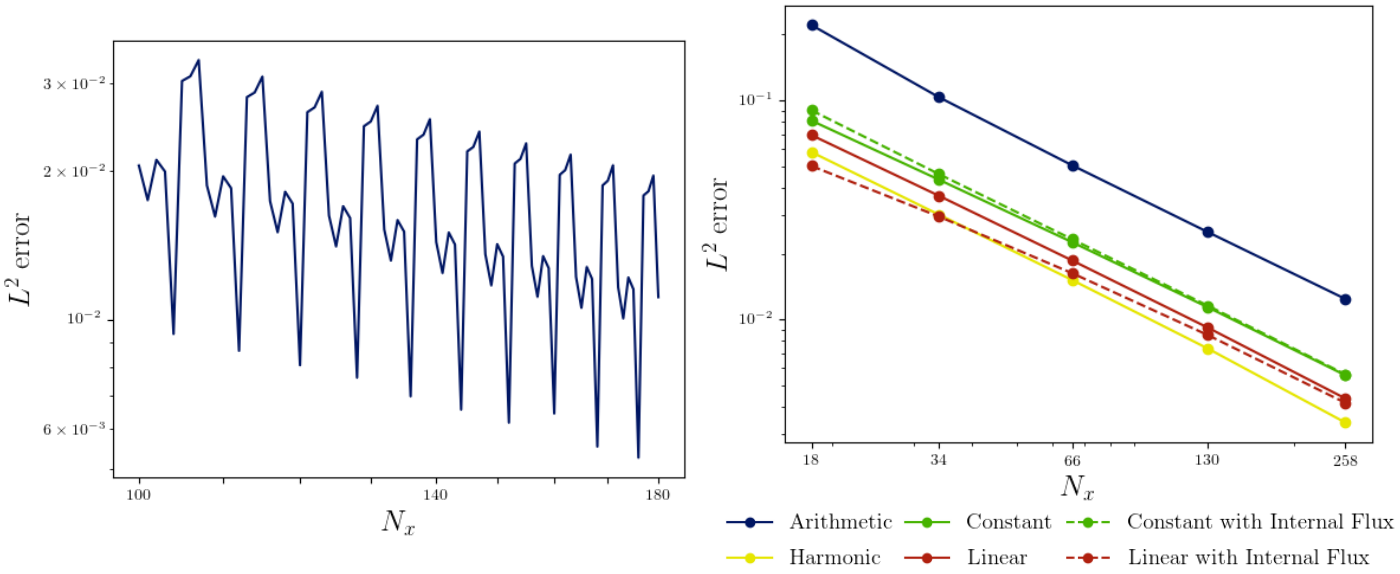

Figure 6: Left: 1D problem errors for the arithmetic homogeneous mean method on different meshes. The number of cell takes every integer value between 100 and 180. Right: 1D problem convergence errors at $N_x \equiv 2[8]$ for different methods and mesh dimensions. The terms "Constant" and "Linear" both refers

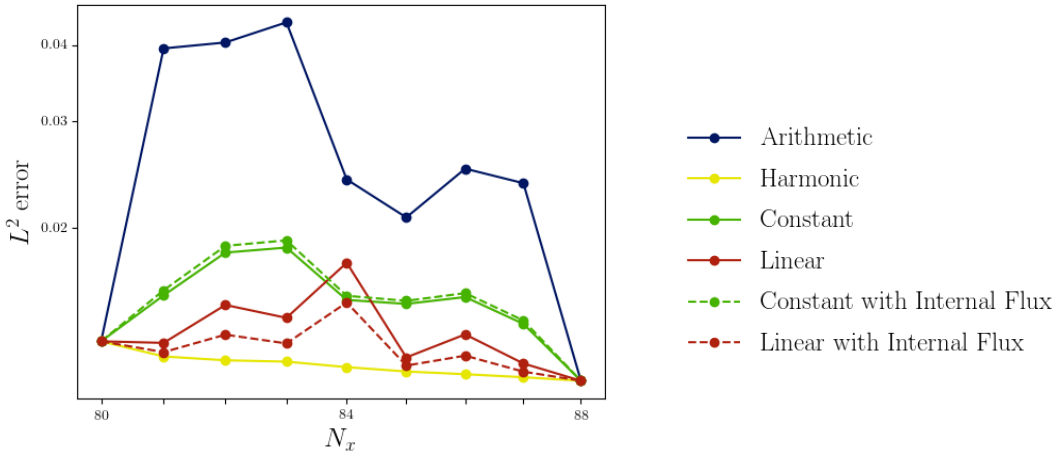

Figure 7: 1D problem modulation errors for different methods and mesh dimensions. The terms "Constant" and "Linear" both refers to the face volume fractions computation method.

underlying geometric considerations seem to be worthy. However, as the mesh is refined, the internal flux effect decreases until being no longer significant. This phenomenon may be explained by the fact that, as mixed cells become smaller, their neighbor (pure) cells get closer in terms of distance and, consequently, in terms of temperature. As a result, the temperatures of the materials inside mixed cells are also closer, thus reducing the need for an internal flux.

Linear computation of the face volume fractions improves the accuracy for values of N_x which

are almost multiple of 8 (or equivalently, for mixed cells with volume fractions close to 1 or 0, i.e. mixed cells that are almost pure cells) in comparison with constant computations. Indeed, linear reconstruction helps to lower the fluxes implicating materials occupying a limited space inside the cell. However, for other values of N_x, the modulation pattern peaks and linear reconstruction methods does not fare well. For more sophisticated problems, it is expected that the set of mixed cells will have various volume fractions. Hence, what eventually matters is the average value of the error or, equivalently, the area under the modulation curve. In that regard, linear reconstruction methods could be preferable. Albeit being a homogeneous method, the harmonic mean method is very accurate, which makes sense because the underlying equivalent thermal conductivities are calibrated in order to give an exact global flux for this particular problem. As for the arithmetic mean, the results are terrible.

3.2 Sand and shale

We now consider the classical sand and shale [7] problem where a domain $[0, 1] \times [0, 0.5]$ of high conductivity $K_1 = 1$ (the sand) is filled with squares of low conductivity $K_2 = 10^{-10}$ material (the shale). The square length is set to 0.05 and are randomly generated inside the domain. Temperature is equal to $T_b = 4$ at the bottom, and $T_t = 0$ at the top. Fluxes are set to zero along the left and right borders. Results of different methods are compared at time $t = 1s$ with a reference computed on a refined mesh (which contains no mixed cell). The maximum adjustment with linear computation of the surface fractions is once again the most effective method. The difference with the neutral adjustment is quite significant, and linear reconstruction also improves slightly the results. The modulation curve is even sub-linear in the sense that it is located under the line joining the two extremities of the modulation curve (i.e where there is no mixed cell and all methods are equivalent). This essentially means that the maximum adjustment is here able to achieve better results with mixed cells than with a higher number of pure cells.

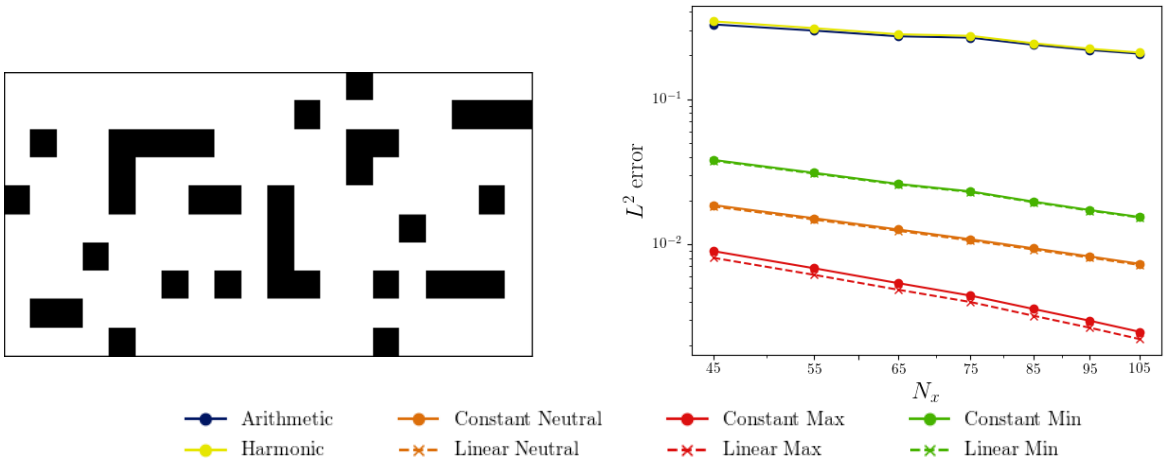

Figure 8: Left:The sand and shale distribution considered. Black blocks corresponds to shale. Right: The two sand and shale problems results with $N_y \equiv 5[10]$.

4 CONCLUSION

This work is mainly motivated by the development of numerical strategies which do not require the use of geometric interface reconstructions for the multimaterial diffusion equation. In this document, a simple diffuse interface strategy is proposed. Different variations of the methodology introduced here have been studied. It seems that the approach with maximum adjustment is, in general, the most accurate. However, the differences observed between the different methods remain relatively small. Therefore, because of its simplicity, we believe that the neutral method (which corresponds to $\lambda = 0$) is recommended for many applications. The numerical test cases presented here show the interest of the methods compared to standard homogeneous ones. Obviously, the drawback of the strategy comes from its accuracy, which can not compete with reconstruction based ones. However, its simplicity and robustness make it particularly attractive.

REFERENCES

[1] M. R. Baer and J. W. Nunziato. A two-phase mixture theory for the deflagration-to-detonation transition in reactive granular materials. *Multiphase Flow*, 12, 861–889, 1986.

[2] J.P. Boris and E.S. Oran. The numerical simulation of compressible reactive flows. *AIAA Papers No., 87-1323*, 1987.

[3] J.W. Cahn and J.E. Hiliard. Free energy of a nonuniform system. *J. Chem. Phys. 28, 258-267*, 1958.

[4] C. Chaigneau. *CEA report*, 1997.

[5] J. GLimm, J.W. Grove, X.L. Li, K.M. Shyue, and Q. Zhang. Three-dimensional front tracking. *J. Sci. Comput, 19, 703-727*, 1998.

[6] S. Karni. Multicomponent flow calculations by a consistent primitive algorithm. *J. Comput. Phys.*, 112, 31, 1994.

[7] E. Kikinzon, Y. Kuznetsov, K. Lopnikov, and M.J. Shashkov. Approximate static condensation algorithm for solving multi-material diffusion problems on mesh non-aligned with material interfaces. *J. Comput. Phys.*, 2017.

[8] V. Maltsev, M. Skote, and P. Tsoutsanis. High-order methods for diffuse-interface models in compressible multi-medium flows: A review. *Physics of Fluids*, 34(2):021301, 2022.

[9] B.D. Nichols and C.W. Hirt. Improved free surface boundary conditions for numerical incompressible-flow calculations. *J. Comput. Phys. 8, 434-448*, 1971.

[10] B.J. Parker and D.L. Youngs. Two and three dimensional eulerian simulations of fluid flow with material interfaces. *Technical Report 01/92*, 1992.

[11] S.O. Unverdi and G. Tryggvason. A front-tracking method for viscous incompressible, multi-fluid flows. *J. Comput. Phys. 100, 25-37*, 1992.